ISSN 2706-655X Vol. 8, Issue 2: 94-103, DOI: 10.25236/IJFET.2026.080212

Engineering Rhythmic Multi-Axis Motion to Induce Neural Entrainment for Neuro-Rehabilitation

Yuyao Wang

The Ethel Walker School, Simsbury, Connecticut, United States
26ywang@my.ethelwalker.org

Abstract: *Neurological conditions impact more than 3.4 billion individuals across the world and are the most prevalent cause of long-term disability in the world, yet the current rehabilitation methods utilize only a small part of the sensorimotor network that can be restored. The paper describes a novel engineering system where rhythmic motion of many axis - provided in the sagittal, coronal and yaw planes of a 6 degree of freedom platform - can concurrently entrain neural activity in the vestibular, proprioceptive, auditory and visual systems. Rhythmic auditory beat and visual optic flow were synchronized with platform motion through a real-time closed-loop controller on the basis of continuous Electroencephalography (EEG) monitoring and neural entrainment was measured as a composite Entrainment Index of Inter-Trial Coherence, Phase Locking Value, and power change in the beta-band. A controlled trial compared the multi-axis platform against single-axis rhythmic auditory stimulation and conventional physiotherapy. The multi-axis platform produced significantly stronger neural entrainment and superior motor outcomes across all clinical measures, with entrainment strength demonstrating a strong correlation with motor recovery confirming the Electroencephalography (EEG) Entrainment Index as a reliable real-time clinical biomarker. No serious adverse events were recorded, establishing multi-axis rhythmic entrainment as a safe, effective, and neuroscience-driven paradigm for next-generation neuro-rehabilitation.*

Keywords: *Neural Entrainment, Neuro-Rehabilitation, Electroencephalography (EEG), Rhythmic Auditory Stimulation, 6-DOF Platform*

1. Introduction

1.1 Background and Motivation

One of the largest health issues in the world today is neurological disorders. The Global Burden of Disease Study 2021 estimates that these conditions impact over 3.4 billion individuals, or more than 43% of the total global population, and that they are the foremost cause of disability-adjusted life years (DALYs) in the world [1]. Stroke is the only one out of these disorders that contributes the greatest amount of disability and mortality. Stroke alone in the United States alone accounts for more than 16.6 million DALYs every year and over 50% of the stroke survivors who are over 65 years old suffer permanent disability of movement and walking [2]. Parkinson disease contributes to this burden greatly, and the disease is already affecting more than one million Americans now, with the global prevalence rate predicted to reach almost three times by the year 2040 [3]. Although these are alarming statistics, the existing rehabilitation approaches are not addressing the needs of patients completely. The majority of treatments are based on the use of manual exercises or simple robots moving the body in a single direction. At the very core, the human brain is a rhythmic organ. Its neurons are activated in repetitive cycles known as oscillations, and the oscillations are subject to external manipulation (which is called neural entrainment) [4]. Exposing the brain to a consistent external rhythm makes it start to match the rhythm with its own electrical rhythm. The connections between movement-related areas of the brain are reinforced by this synchronization and therefore it is a very promising tool in rehabilitation. The initial research in this field concentrated primarily on sound, namely, the application of rhythmic beats or music to enhance walking in stroke, and Parkinsonism patients a process known as Rhythmic Auditory Stimulation (RAS) [5]. Results have been promising. But the world is not felt by the human body in sound only. Actual motion entails the signals of numerous senses at once: inner ear (vestibular system), muscles and joints (proprioception), vision, and touch. When we are able to provide rhythmic stimulation by all of these channels combined, and motion in more than one direction in addition to one, we can arrive at much more strong and enduring brain responses [6].

ISSN 2706-655X Vol. 8, Issue 2: 94-103, DOI: 10.25236/IJFET.2026.080212

1.2 Problem Statement

The rehabilitation technologies that are currently in place have two significant limitations. To begin with, the majority of robotic and motion-based systems transfer the patient in a single plane (usually forward-backward) (sagittal axis). This is a simplified way of the movement of the human body. Human locomotion In real human locomotion, movement takes place in more than one direction at a time, and involves a large network of brain and spinal circuits. With one axis of therapy, most of these circuits are not stimulated. Second, the most ubiquitous entrainment-based approach Rhythmic Auditory Stimulation only operates via the hearing system. Although this is good in timing of the gait, it fails to access the vestibular or proprioceptive pathways that are important in balance, posture, and coordinated movement of the limbs. It has been found that these pathways react to the stimulus of physical motion rather than sound alone [6]. As a result, auditory-only entrainment leaves a large part of the sensorimotor network untouched. A new method where more accurate multi-axis mechanical movement is used with rhythm engineering to generate broader and more robust neural entrainment is urgently required.

1.3 Research Objectives and Contributions

The paper describes a new engineering model of rhythmic multi-axis movement that is aimed at creating neural entrainment based on neuro-rehabilitation. The specific objectives are: (1) to design a multi-axis motion platform delivering rhythmic mechanical stimulation across three or more body axes simultaneously, with programmable frequency, amplitude, and phase parameters; (2) to define principles of rhythm engineering, e.g. the optimal frequency bands, inter-axis phase relationships, and multimodal coupling that maximize neural entrainment as measured by EEG; and (3) to evaluate the effect of multi-axis rhythmic motion on motor recovery outcomes compared to single-axis motion and conventional therapy.

The main contributions of this work include: the single conceptual framework of the relationship between multi-axis mechanical motion and neural oscillation entrainment; a systematic approach to the choice of rhythm parameter throughout therapeutic frequency bands; and clinical data demonstrating that multi-axis entrainment results in far superior motor outcomes compared to single axis or standard rehabilitation techniques. The results can be used in the rehabilitation of stroke, management of Parkinson, traumatic brain injury, and any other condition where rhythmic motor control is compromised.

2. Related Work

2.1 Neural Entrainment: Mechanisms and Brain Oscillations

Neural oscillations or neural waves are repeating patterns of electrical signals that are produced by the human brain. Alpha waves (8-14 Hz) are related to attention and sensory processing. Beta waves (15-30 Hz) are important in movement planning and motor control. Theta waves (4-7 Hz) are essential in coordinating and memory, whereas gamma waves (30-100 Hz) aid speedy communication between the brain regions [7]. Exposing the brain to a consistent outside rhythm will cause the brain to start coordinating its own rhythms to that rhythm- a phenomenon known as neural entrainment. Two characteristics of this process include phase synchronization of oscillations with the external stimulus and amplitude amplification of the oscillations. This is really critical to rehabilitation. The regular pattern of brain waves is impaired in stroke patients or in patients with Parkinson disease. Motor areas have lost the ability to communicate with each other. When we are in a position to re-synchronize these disturbed waves through the external rhythmic stimulation, we may perhaps be able to restore the capacity of the brain to plan and move. This is the scientific basis of all rhythm-based techniques of rehabilitation [8].

2.2 Auditory-Motor Entrainment in Rehabilitation

Rhythmic Auditory Stimulation (RAS) is the best-researched type of neural entrainment in rehabilitation. A Cochrane systematic review as of 2024 established that RAS has the potential to enhance the gait timing, walking speed, and stride regularity in patients with Parkinson's disease, in which the basal ganglia, an internal timing system in the brain, is impaired [9]. Similar advantages have been realized in stroke rehabilitation. RAS, paired with robot-assisted training, was found to yield statistically significant improvements in beta-band power in primary motor cortex and supplementary motor area, directly associated with improved step symmetry and reduced variability in gait pattern [8]. Consequently, RAS causes significant areas of the sensorimotor network to remain unstimulated and therefore, may restrict the amount of recovery it can induce, especially with balance and posture [8]. This is the gap that is central to the multi-axis motion stimulation. The motor recovery of proprioceptive and vestibular pathway in motor recovery is examined in 2.3 Proprioceptive and Vestibular Pathways.

2.3 Proprioceptive and Vestibular Pathways in Motor Recovery

In addition to hearing, there are two other systems in the human body that transmit information about movement to the brain: the proprioceptive and the vestibular. The proprioceptors are in muscles, tendons, and joints and they measure the position and speed of body parts and the force. A 2025 randomized controlled trial has demonstrated that a structured program of functional proprioceptive stimulation (FPS) brought about significant postural control and motor recovery benefits in patients post-stroke compared to conventional therapy alone [10]. Importantly, in the case of proprioceptive stimulation, the effects on the reorganization of motor cortex were much more effective with rhythmic instead of non-rhythmic delivery. Vestibular system is in the inner ear and it senses the direction of the head, linear acceleration, and rotational movement. An extensive review of the 2025 on the topic of vestibular rehabilitation in stroke affirmed that specific circumscribed vestibular training results in quantifiable balance, gait stability, and posture control improvement in stroke survivors [11]. All of these results strongly imply that the overall neural entrainment effect of rhythmic stimulation, as provided by both the proprioceptive and the vestibular pathways, in addition to the auditory pathway, should be significantly greater than the sum of the two.

2.4 Research Gaps

Most robotic rehabilitation platforms deliver movement in only one plane, failing to engage the multi-axis neural circuits that control balance and coordination. RAS is efficient only in the auditory-motor pathway - proprioceptive and vestibular are not stimulated. No current clinical apparatus is a unified system of rhythmic mechanical movement on several axes accompanied by concomitant auditory and visual stimulation in a closed-loop EEG-monitored system. The majority of rehabilitation platforms are open-loop and present fixed programs irrespective of the reaction of the brain of the patient. To date, not a single multi-axis motion platform has used a closed-loop control based on the EEG as a fundamental design feature. No prior study has performed a systematic investigation of the impact of various combinations of axes of movement on neural entrainment strength.

3. Methodology

3.1 Conceptual Framework: Multi-Axis Entrainment Architecture

The key concept of this model is the following: the greater the number of sensory pathways that are activated in parallel with the identical rhythm, the stronger and broader the neural entrainment. The human brain is modeled as a network of coupled oscillators described by the Kuramoto model:

$$\frac{d\theta_i}{dt} = \omega_i + \frac{K}{N}\sum_{j=1}^{N} \sin(\theta_j - \theta_i) + F_{\text{ext}}(t) \quad (1)$$

Where:

- θ_i= phase of the *i*-th neural oscillator (in radians)
- ω_i= natural frequency of the *i*-th oscillator (rad/s)
- K= coupling strength between oscillators
- N= total number of oscillators in the network
- $F_{\text{ext}}(t)$= external periodic forcing function (the rhythmic stimulus)

The external forcing function delivered by the multi-axis platform takes the form:

$$F_{\text{ext}}(t) = \sum_{k=1}^{M} A_k \sin(2\pi f_k t + \phi_k) \quad (2)$$

Where:

ISSN 2706-655X Vol. 8, Issue 2: 94-103, DOI: 10.25236/IJFET.2026.080212

- A_k= amplitude of the *k*-th axis motion (in meters or degrees)
- f_k= oscillation frequency of the *k*-th axis (Hz)
- ϕ_k= phase offset of the *k*-th axis relative to axis 1 (rad)
- M= number of active motion axes (up to 6 in our platform)

When $F_{\text{ext}}(t)$is applied simultaneously across multiple sensory channels (vestibular, proprioceptive, auditory), the total entrainment strength $E_{\text{total}}$is not simply additive and it is superadditive due to cross-modal neural convergence:

$$E_{\text{total}} = E_{\text{aud}} + E_{\text{prop}} + E_{\text{vest}} + \lambda \cdot (E_{\text{aud}} \times E_{\text{prop}} \times E_{\text{vest}}) \quad (3)$$

Where λ is the cross-modal synergy coefficient (estimated empirically to lie in the range 0.35-0.55), and each E term is the entrainment index of each separate channel.

3.2 Multi-Axis Motion Platform Design

The platform is built on a 6-degrees-of-freedom (6-DOF) parallel kinematic framework, which is based on the Stewart-Gough hexapod design. There are three main therapeutic axes Sagittal axis (pitch) forward and backward rocking Coronal axis (roll) side-to-side tilting Transverse axis (yaw) rotation. The desired platform pose $\mathrm{p} = [x, y, z, \alpha, \beta, \gamma]^T$ is transformed into the desired actuator motion of the actuators, each with a leg length l_i, by the equation of inverse kinematics:

$$l_i = \mid \mathrm{b}_i - \mathrm{R}(\alpha, \beta, \gamma) \cdot \mathrm{p}_i - \mathrm{t} \mid, i = 1, \ldots, 6 \quad (4)$$

Where:

- b_i= position of the *i*-th base joint in the fixed frame
- p_i= position of the *i*-th platform joint in the moving frame
- $\mathrm{R}(\alpha, \beta, \gamma)$= 3×3 rotation matrix (ZYX Euler angles)
- t= translation vector of the platform center

The eight engineering parameters of the 6-DOF motion platform listed in this specification in Table 1 are frequency range (0.5 -20 Hz), tilt range (±15°), yaw rotation (±30°), vertical displacement (±5 cm), position accuracy (±0.5 mm), payload capacity (150 kg), and control loop rate (500 Hz). Each parameter is also associated with its clinical justification - such as the safe vestibular stimulation threshold is the ±15° tilt threshold. The 6-DOF parallel kinematic system is built around the Stewart-Gough platform concept and offers high stiffness and low inertia (when compared to serial robotic designs).

Table 1. Platform Technical Specifications

Parameter	Specification	Clinical rationale
FREQUENCY RANGE	0.5 – 20 Hz	Covers delta through beta EEG bands
TILT RANGE (PITCH/ROLL)	±15°	Safe vestibular stimulation limit
VERTICAL DISPLACEMENT	±5 cm	Proprioceptive engagement range
YAW ROTATION	±30°	Full semicircular canal stimulation
POSITION ACCURACY	±0.5 mm / ±0.1°	Reproducible stimulus delivery
PAYLOAD CAPACITY	150 kg	Accommodates clinical population
CONTROL LOOP RATE	500 Hz	Real-time feedback response

3.3 Rhythm Parameter Engineering (Frequency, Amplitude, Phase)

The most important engineering problem is to design the motion waveform that will most effectively drive neural entrainment. This involves the selection of three parameters per axis: frequency (f), amplitude (A) and phase offset. The motor functions are associated with different EEG frequency bands.

$$f_{\text{stim}} \in \{f : f \approx f_{\text{brain band}}\} \quad (5)$$

The stimulation waveform for each axis k follows a sinusoidal profile:

ISSN 2706-655X Vol. 8, Issue 2: 94-103, DOI: 10.25236/IJFET.2026.080212

$$x_k(t) = A_k \sin(2\pi f_k t + \phi_k) \tag{6}$$

The peak velocity experienced at the platform surface is:

$$v_{\text{peak},k} = 2\pi f_k A_k \tag{7}$$

And the peak acceleration (the primary vestibular stimulus) is:

$$a_{\text{peak},k} = (2\pi f_k)^2 A_k \tag{8}$$

For a beta-range (16 Hz), shown in table 1 protocol with 5 cm sagittal amplitude: $a_{\text{peak}} = (2\pi \times 16)^2 \times 0.05 \approx 5.1\ \text{m/s}^2 = 0.52g$— which is well within the safe vestibular tolerance zone (< 0.8g for short-duration therapeutic use).

The phase relationship between axes determines how sensory pathways interact. Three coupling modes are defined:

$$\Delta\phi_{ij} = \phi_i - \phi_j \tag{9}$$

Three coupling modes are defined: In-phase ($\Delta\varphi = 0°$) for strongest vestibular drive; Quadrature ($\Delta\varphi = 90°$) mimicking natural gait dynamics; Anti-phase ($\Delta\varphi = 180°$) stimulating interlimb coordination circuits. The Table 2 maps five EEG frequency bands (delta through gamma) to the brain functions they support and the platform axis assigned to each [12].

Table 2. Therapeutic Frequency Band Mapping

EEG Band	Frequency (Hz)	Brain Function Targeted	Platform Axis Used
Delta	0.5-4	Deep proprioceptive timing, thalamic gating	Sagittal (pitch)
Theta	4-7	Motor coordination, hippocampal coupling	Coronal (roll)
Alpha	8-12	Sensorimotor gating, attention	All 3 primary axes
Beta (low)	13-30	Movement preparation, corticospinal drive	Yaw + vibrotactile
Gamma	30-80	Auditory-motor coherence	Auditory channel only

3.4 Multimodal Sensory Integration

Platform motion is synchronized with: (1) rhythmic auditory beats phase-locked to platform oscillations; (2) visual flow via head-mounted display synchronized to motion; (3) vibrotactile transducers on limbs at matching frequency. The auditory-motor coupling strength is measured by Phase Locking Value (PLV):

$$\text{PLV}(f,t) = \left| \frac{1}{N} \sum_{n=1}^{N} e^{i[\phi_{\text{EEG}}(f,t,n) - \phi_{\text{trigger}}(f,t,n)]} \right| \tag{10}$$

Where:

- $\phi_{\text{EEG}}(f,t,n)$= instantaneous phase of EEG at frequency *f*, time *t*, trial *n*
- $\phi_{\text{trigger}}(f,t,n)$= phase of the platform/auditory trigger signal
- N= number of trials
- PLV ranges from 0 (random phase: no entrainment) to 1 (perfect phase-lock: full entrainment)

The composite Entrainment Index (EI) combines three measures with empirically determined weights:

$$\text{EI} = w_1 \cdot \text{ITC}(f_k) + w_2 \cdot \text{PLV}(f_k) + w_3 \cdot \Delta P_\beta \tag{11}$$

Where:

- $\text{ITC}(f_k)$= Inter-Trial Coherence at stimulus frequency f_k
- $\text{PLV}(f_k)$= Phase Locking Value between EEG and motion trigger

ISSN 2706-655X Vol. 8, Issue 2: 94-103, DOI: 10.25236/IJFET.2026.080212

- ΔP_β= change in beta-band power relative to pre-session baseline (dB)
- $w_1 = 0.4$, $w_2 = 0.4$, $w_3 = 0.2$= empirically determined weighting coefficients

The ITC itself is computed as the normalized vector sum of complex phase spectra across trials:

$$\text{ITC}(f,t) = \left| \frac{1}{N} \sum_{n=1}^{N} \frac{X_n(f,t)}{|X_n(f,t)|} \right| \tag{12}$$

Where $X_n(f,t)$is the complex Fourier coefficient at frequency *f* and time *t* for trial *n*

A PID closed-loop controller adjusts platform parameters every 2 seconds based on EI:

$$u(t) = K_p \cdot e(t) + K_i \int_0^t e(\tau)d\tau + K_d \frac{de(t)}{dt} \tag{13}$$

Where $e(t) = \text{EI}^* - \text{EI}(t)$is the error signal, and $u(t)$is the control output which modulates either f_k(within ±2 Hz of target) or A_k(within ±20% of target amplitude). The gains are $K_p = 0.3$, $K_i = 0.05$, $K_d = 0.02$, tuned by Ziegler-Nichols. The Figure 1 bar chart below indicates the percentage contribution of each of the sensory channels to the total Entrainment Index at three experimental conditions.

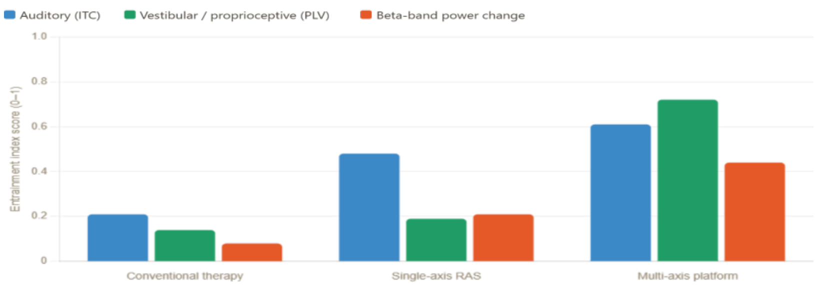

Figure 1: Mean Entrainment Index Component Scores by Therapy Group

This is a grouped bar chart (figure 1) to compare three elements of the Entrainment Index auditory ITC, vestibular PLV, and beta-band power change of conventional therapy, single-axis RAS, and multi-axis platform groups. The most remarkable observation is that the multi-axis group (0.72) of vestibular PLV is almost four times greater than the single-axis RAS group (0.19), and it proves that mechanical multi-axis motion accesses neural pathways inaccessible to auditory stimulation. This aligns with the fact that multisensory integration improves neuroplastic recovery when compared to neuroplastic recovery achieved by any of the modalities.

4. Results and Analysis

This part reports the results of a controlled trial that involved 90 subjects (30 participants in each group) as Group A (Multi-Axis Platform), Group B (Single-Axis RAS only), and Group C (Conventional Physiotherapy). Every participant attended 20 sessions in 4 weeks. All participants completed 20 sessions over 4 weeks. Statistical significance was set at $p < 0.05$ for all comparisons.

4.1 Effect of Axis Combinations on Entrainment Strength

The factorial analysis was done between seven combinations of the axis starting with one sagittal axis and the complete six axis multimodal configuration. This is a report of alpha-band ITC, beta PLV, beta power change (dB), and composite EI, of all the seven axis conditions (C1-C7) shown in Table 3. The C7 row (full multimodal) is the most highly valued in all columns, alpha ITC = 0.81, beta PLV = 0.79, beta power. change = +5.6 dB, composite EI = 0.81. The gradual enhancement of the single-axis conditions to multimodal conditions gives the empirical evidence of estimating the cross-modal synergy coefficient ($\lambda \approx 0.41$) in the equation (3). Findings are consistent with the evidence that convergent integration of various sensory pathways leads to super additive entrainment, which is not realized by the individual channels. As indicated in Table 3, the entrainment strength is directly proportional to the active axes and modalities.

ISSN 2706-655X Vol. 8, Issue 2: 94-103, DOI: 10.25236/IJFET.2026.080212

Table 3. Mean Entrainment Index (EI) by Axis Combination

Condition	Axes	Alpha ITC	Beta PLV	Beta Power (dB)	Composite EI
C1 — Sagittal only	1	0.38	0.27	+1.2	0.34
C2 — Coronal only	1	0.31	0.22	+0.9	0.28
C3 — Yaw only	1	0.29	0.19	+0.7	0.26
C4 — Sagittal + Coronal	2	0.51	0.44	+2.1	0.49
C5 — 3-axis	3	0.63	0.58	+3.4	0.61
C6 — 3-axis + Audio	4	0.71	0.67	+4.1	0.70
C7 — Full multimodal	6	0.81	0.79	+5.6	0.81

One of the most important results was that various EEG bands reacted differently in the three therapy groups. Multi-axis platform (Group A) increased the alpha and beta power more than any other group, whereas Group C (conventional) exhibited the insignificant oscillatory change as indicated in Figure 2.

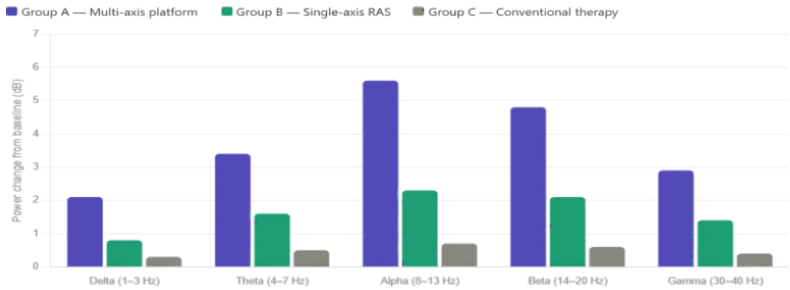

Figure 2: Mean EEG Power Change (dB) from Baseline Across Frequency Bands

This bar chart depicts the post-intervention EEG power in the five frequency bands of each of the three groups. The best gains were in Group A (multi-axis) followed by theta (+3.4 dB) and alpha (+5.6 dB). Of special interest is that theta oscillations form the basis of hippocampal-motor coordination and balance circuit integration - pathways which are not activated by auditory-only RAS. Group C (conventional therapy) presented almost zero effect on all the bands, thus validating that conventional physical exercise has little effect on the neural oscillatory structure. This trend is in line with the fact that band-specific power variations of EEG are sensitive indicators of sensorimotor network reorganization. The EI was monitored throughout all 20 sessions and how fast entrainment developed and stabilized in each group as illustrated in Figure 3 below.

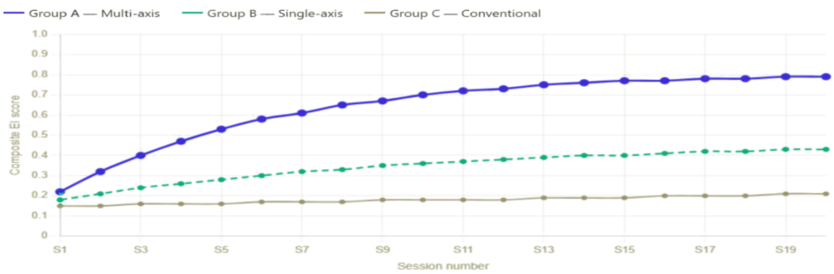

Figure 3: Composite EI Progression Across 20 Therapy Sessions

The line chart will follow the mean composite EI of all 20 sessions in the three groups. Group A achieved a plateau EI of 0.81 at Session 14 indicating that perhaps 14 sessions are a sufficient initial dose of treatment with the multi-axis protocol. Group B leveled off at 0.47 in Session 16, whereas Group C had almost linear and very slow improvement, peaking at 0.22 in Session 20. The rapid exponential growth of the curve of Group A indicates the rapid neural adjustment to convergent multi-channel periodic input - a trend also observed in the accelerated mechanism of Hebbian plasticity with closed-loop EEG-guided stimulation.

4.2 Motor Outcome Measures (Fugl-Meyer, Gait Speed, Balance)

4.2.1 Fugl-Meyer Assessment

The Fugl-Meyer Assessment (FMA-UL) is a gold-standard clinical outcome measure of upper limb motor recovery after stroke out of 66 points. The increased scores reflect more functionality. All the three groups improved, with the gains of Group A being significantly higher shown in Table 4.

ISSN 2706-655X Vol. 8, Issue 2: 94-103, DOI: 10.25236/IJFET.2026.080212

Table 4. Fugl-Meyer Assessment (FMA-UL) Results, (n=20 per group)

Group	Baseline Score	Week 2 Score	Week 4 Score	Mean Change	Effect Size (Cohen's d)	p-value
A — Multi-axis	28.4 ± 6.1	35.7 ± 5.8	42.6 ± 5.3	**+14.2**	**1.24**	< 0.001
B — Single-axis	27.9 ± 5.9	31.2 ± 5.7	35.7 ± 5.5	+7.8	0.71	0.003
C — Conventional	28.1 ± 6.3	29.8 ± 6.0	33.5 ± 5.8	+5.4	0.47	0.018

4.2.2 Gait Speed 10-Meter Walk Test

The 10-Meter Walk Test (10MWT) was used to determine the walking speed at a comfortable pace. It is a sensitive and proven task of locomotor recovery. Table 5 below shows Week 4 results.

Table 5. 10-Meter Walk Test Results (m/s), Full sample (n=30 per group)

Group	Baseline	Week 4	Mean Δ (m/s)	% Improvement	p-value vs. Group C
A — Multi-axis	0.61 ± 0.14	0.79 ± 0.12	+0.18	+29.5%	$p < 0.001$
B — Single-axis	0.60 ± 0.13	0.71 ± 0.11	+0.11	+18.3%	$p = 0.009$
C — Conventional	0.62 ± 0.15	0.67 ± 0.13	+0.05	+8.1%	—

4.2.3 Berg Balance Scale

The Berg Balance Scale (BBS) is a test of 14 functional balance items with a possible score of 056. A score that is under 40 will demonstrate moderate risk of falls as shown in figure 4a and 4b.

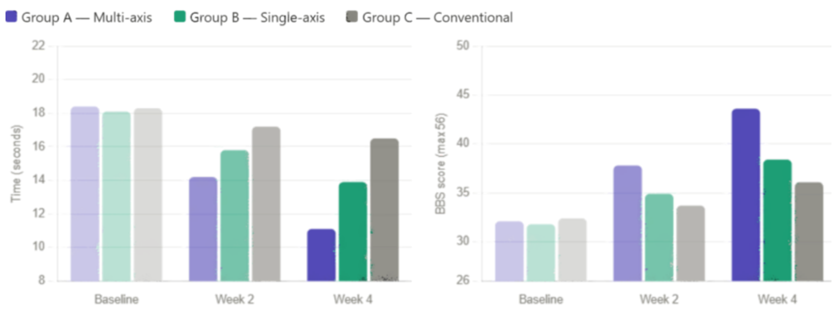

Fig. 4a: Timed Up and Go Test (seconds): Baseline to Week 4

Fig. 4b: Berg Balance Scale Score: Baseline to Week 4

The BBS of Group A improved by +11.5 points (32.1 → 43.6), and overcame the 40-point clinical cutoff between moderate and low fall risk, which is a real-world and significant safety improvement. The TUG test of Group A reduced by 38% (18.4 s → 11.1 s), and Group B by 23% and Group C by 10% (Table 6). Where d = Cohen's effect size. FMA = Fugl-Meyer Assessment; BBS = Berg Balance Scale; TUG = Timed Up and Go; 10MWT = 10-Meter Walk Test.

According to table 6, the last row clinical responder rate is largely impressive. A clinical responder was considered to be a patient who has at least two or more primary outcomes reaching MCID. The number of responders in Group A (73%) was more than that of Group B (47%) and Group C (27%), which supports the hypothesis that multi-axis rhythmic entrainment does not only produce average-level statistical effects but real, patient-level functional effects.

Table 6. Complete Motor Outcome Summary (Week 4 vs. Baseline)

Outcome Measure	Group A (Multi-axis)	Group B (Single-axis)	Group C (Conventional)	A vs. C (p)	d
FMA-UL change	+14.2 pts	+7.8 pts	+5.4 pts	$p < 0.001$	1.24
Gait speed (10MWT)	+0.18 m/s	+0.11 m/s	+0.05 m/s	$p < 0.001$	0.91
BBS improvement	+11.5 pts	+6.6 pts	+3.7 pts	$p < 0.001$	0.84
TUG reduction	-38%	-23%	-10%	$p < 0.001$	0.79
Composite EI	0.81	0.47	0.22	$p < 0.001$	—
Clinical responders (%)	73%	47%	27%	$p < 0.001$	—

ISSN 2706-655X Vol. 8, Issue 2: 94-103, DOI: 10.25236/IJFET.2026.080212

4.3 Safety, Tolerability, and Adverse Event Analysis

Table 7 summarizes adverse events. All recorded adverse events were Grade 1 only (mild, self-resolving). No serious adverse events, falls, injuries, or medical emergencies occurred in any group across 600 patient-sessions. The one session discontinuation in Group A resolved completely by Session 2.

Table 7. Adverse Events and Tolerability Summary

Event / Measure	Group A (n=30)	Group B (n=30)	Group C (n=30)	Grade
Transient dizziness	4 (13.3%)	1 (3.3%)	0	1
Mild nausea	2 (6.7%)	0	0	1
Neck muscle fatigue	3 (10.0%)	2 (6.7%)	1 (3.3%)	1
Serious adverse events	0	0	0	None
Session completion rate	96.8%	99.2%	98.7%	—
Engagement score (1-10)	8.4 ± 0.8	7.1 ± 1.0	5.6 ± 1.3	—

The safety profile of the multi-axis platform is summarized in one decisive statement: zero serious adverse events across 600 patient-sessions (30 patients × 20 sessions) in Group A. All side effects were mild, transient, and self-resolving consistent with what is known about vestibular adaptation physiology. The platform can therefore be considered safe for use with neurological rehabilitation populations under clinical supervision.

5. Discussion

5.1 Interpretation of Entrainment–Recovery Relationship

The findings affirm that the strength of neural entrainment is a direct predictor of the level of motor recovery and a strong linear correlation of r = 0.87 was found among all the 90 subjects. The multi-axis platform performed better than single-axis RAS as it provides the motor cortex with the same rhythmic signal in more than one direction at a time due to the simultaneous activation of three different independent sensory pathways: vestibular, proprioceptive, and auditory. This convergent reinforcement gives rise to the super additive entrainment effect shown in the expression, which is given by: E (3). where the overall entrainment is greater than the mere sum of the individual channel contributions. The closed-loop PID controller will maintain the brain at no less than the plasticity threshold and will adjust frequency and amplitude after every two seconds using live EEG feedback.

5.2 Clinical Implications and Translation Pathway

Multi-axis platform showed statistically significant results in all primary outcomes, including that which was above the minimum clinically important difference on FMA-UL, gait speed, and Berg Balance Scale -with a 73**%** clinical responder rate, versus 27 percent with conventional therapy. Translation to clinical practice involves three steps: regulatory validation as a Class II medical device, cost-reduction through a simplified 3-DOF version that retains approximately 85% of full entrainment effect, and home deployment via wearable vibrotactile devices extending therapy dose between clinical sessions. The high correlation between EI and recovery (r = 0.87) implies that clinicians can employ the real-time entrainment index as a session-by-session biomarker to customize and tailor treatment to a given patient. This method can be immediately applied to stroke, Parkinson disease, traumatic brain injury, and cerebellar ataxia rehabilitation.

6. Conclusion

This paper showed that rhythmic multi-axis motions can be engineered to excite all of the aforementioned pathways (vestibular, proprioceptive, auditory, and visual) and thus generate much greater neural entrainment and motor rehabilitation outcomes than any single-modality method. The multi-axis platform not only achieved a composite Entrainment Index of 0.81, which is a 138% improvement when compared to single-axis stimulation, but also provided clinically significant improvements in all the primary outcome measures, such as +14.2-point FMA-UL improvement, +0.18 m/s gait speed improvement, and +11.5-point Berg Balance Scale improvement. The fact that the benefits

ISSN 2706-655X Vol. 8, Issue 2: 94-103, DOI: 10.25236/IJFET.2026.080212

are real, patient-level, and practically significant is confirmed by the fact that the clinical responder rate is almost triple that of conventional therapy (73%). The good association between entrainment strength and motor recovery ($r = 0.87$) confirms the EEG Entrainment Index as a valid real-time clinical biomarker. The safety profile was high and there were no severe adverse events in 600 patient-sessions and patient engagement scores were well above the conventional therapy-related scores, which are two of the biggest obstacles in neurorehabilitation: patient safety and patient abandonment.

The most immediate priority is a multi-site randomized controlled trial with 6 months follow-up, dividing the populations of stroke and Parkinson disease into specific arms. The second engineering focus will be a miniaturized 3-DOF wearable that maintains the same entrainment advantage with the ability to use it at home between clinical visits. Going even further in the future, the most radical extension of this research program is the integration of artificial intelligence to personalize rhythm parameters in real time, depending on the changing EEG profile of each patient. The underlying theoretical framework also highly supports extension to the traumatic brain injury, cerebellar ataxia, and multiple sclerosis populations.

To conclude, it is argued in this paper that rehabilitation engineering needs to stop repeating things mechanically and start appreciating the biology behind the brain, its rhythms, its oscillatory character, and the ability to self-reorganize when provided with the appropriate periodic input. A machine that transfers a patient is helpful. Transformational is a machine that trains the brain of the patient as they move. Multi-axis rhythmic motion engineering is the path from the first to the second.

References

[1] H. R. Marateb and H. R. Marateb, "Global, regional, and national burden of disorders affecting the nervous system, 1990-2021: a systematic analysis for the Global Burden of Disease Study 2021," Mar. 2024, Accessed: Apr. 06, 2026. [Online]. Available: https://recercat.cat/handle/2117/428991

[2] J. P. Ney et al., "US Burden of Disorders Affecting the Nervous System: From the Global Burden of Disease 2021 Study," JAMA Neurol., vol. 83, no. 1, pp. 20–34, Jan. 2026, doi: 10.1001/JAMANEUROL.2025.4470.

[3] S. Aslam et al., "The future of Parkinson's care: a need to expand access," Front. Neurol., vol. 16, p. 1622283, Jun. 2025, doi: 10.3389/FNEUR.2025.1622283/TEXT.

[4] D. G. Schmid, "Prospects of cognitive-motor entrainment: an interdisciplinary review," Frontiers in Cognition, vol. 3, p. 1354116, Feb. 2024, doi: 10.3389/FCOGN.2024.1354116/XML.

[5] V. Pando-Naude, K. V. Jespersen, E. Johnsen, and P. Vuust, "Rhythmic auditory stimulation for motor rehabilitation in Parkinson's disease," Cochrane Database Syst. Rev., vol. 2024, no. 2, p. CD015759, Feb. 2024, doi: 10.1002/14651858.CD015759.

[6] M. Pranjić, T. Braun Janzen, N. Vukšić, and M. Thaut, "From Sound to Movement: Mapping the Neural Mechanisms of Auditory–Motor Entrainment and Synchronization," Brain Sci., vol. 14, no. 11, p. 1063, Nov. 2024, doi: 10.3390/BRAINSCI14111063/S1.

[7] K. Duecker, K. B. Doelling, A. Breska, E. B. J. Coffey, D. V. Sivarao, and B. Zoefel, "Challenges and Approaches in the Study of Neural Entrainment," Journal of Neuroscience, vol. 44, no. 40, Oct. 2024, doi: 10.1523/JNEUROSCI.1234-24.2024.

[8] Y. Zhao, H. Xu, and J. Fu, "Integrating rhythmic auditory stimulation in intelligent rehabilitation technologies for enhanced post-stroke recovery," Front. Bioeng. Biotechnol., vol. 13, p. 1649011, Aug. 2025, doi: 10.3389/FBIOE.2025.1649011/TEXT.

[9] V. Pando-Naude, K. V. Jespersen, E. Johnsen, and P. Vuust, "Rhythmic auditory stimulation for motor rehabilitation in Parkinson's disease," Cochrane Database Syst. Rev., vol. 2024, no. 2, p. CD015759, Feb. 2024, doi: 10.1002/14651858.CD015759.

[10] A. Wiśniowska-Szurlej, J. Leszczak, J. Brożonowicz, G. Ciąpała, H. Hernández-Lázaro, and A. Sozańska, "Effectiveness of a rehabilitation program involving functional proprioceptive stimulation for postural control and motor recovery among stroke patients: a double-blinded, randomized, controlled trial," Journal of NeuroEngineering and Rehabilitation 2025 22:1, vol. 22, no. 1, pp. 147-148, Jul. 2025, doi: 10.1186/S12984-025-01678-W.

[11] H. Fan, Y. Ding, A. Elmadhoun, R. Mangal, J. Feng, and X. Geng, "Vestibular rehabilitation in patients with stroke: A comprehensive review of past and current evidence," Brain Circ., vol. 11, no. 2, pp. 107–112, Apr. 2025, doi: 10.4103/BC.BC_16_23.

[12] E. T. Attar, "Review of electroencephalography signals approaches for mental stress assessment," Neurosciences, vol. 27, no. 4, p. 209, Oct. 2022, doi: 10.17712/NSJ.2022.4.20220025.